

# Dynamic photonic textiles for personal thermal regulation

*Muluneh G. Abebe and Bjorn Maes*

*Micro- and Nanophotonic Materials Group, Research Institute for Materials Science and Engineering, University of Mons, 20 Place du Parc, B-7000 Mons, Belgium*

More than half of the energy consumed globally is used to heat and cool largely empty residential and commercial buildings. Therefore, more localized heating and cooling efforts are essential. Personal radiative heat regulation by photonic-engineered textiles can help contribute to a more sustainable energy use by expanding the range of comfortable ambient conditions. Recently, various materials and photonic technologies were deployed to design dual-mode dynamic thermoregulating textiles. Generally, two approaches are used: modulating the transmission through the fabric or tailoring the emission from the fabric surface. Here, we propose one design for each approach and discuss their thermal regulation capabilities. In the first design, we employ metal-coated filaments with stimuli-responsive polymer beads to dynamically control the transmission. The second design uses metal nanowires dispersed in a shape-memory-polymer membrane, which form islands upon a highly emissive layer, in order to modulate the emission to the ambient. Both designs provide comfort over a large temperature window, leading to a large potential decrease in heating and cooling costs.

## Introduction

As humanity begins to experience the consequences of climate change, natural disasters due to extreme weather conditions, including a profound impact on public health, have become frequent events in some parts of the world, with growing evidence suggesting that these events are directly related to global warming [1]. Globally, more than half of the energy consumed is used in commercial and residential buildings for heating and cooling purposes [2]. Interestingly, we continuously heat and cool large buildings in order to keep the occupants in thermal comfort, while there is no difference in energy consumption between a few or many occupants. Therefore, a large amount of energy is wasted. This not only contributes to climate change, but also impacts public health by

increasing energy costs, temperature fluctuations, and air pollution, which can result in respiratory and cardiovascular-related diseases [3].

To address this issue and mitigate its impact, shifting towards more localized heating and cooling solutions is crucial [4]. These solutions include innovative approaches like heated chairs, leg warmers, directed heating systems, and photonic thermoregulating textiles [5]. Therefore, by replacing or limiting the use of traditional heating and cooling systems, we can combat climate change and promote better public health outcomes by reducing pollution and costs.

The human body loses its metabolically generated heat through different heat transfer mechanisms such as conduction, convection, evaporation, and radiation (Fig. 1a). However, the contribution of these heat loss channels varies according to the

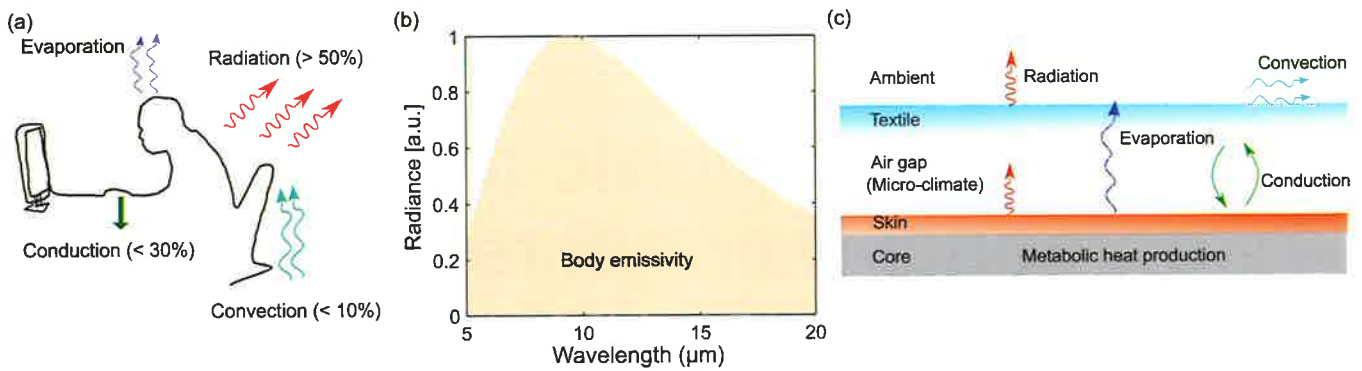


**Figure 1:** (a) Heat dissipation routes of the human body. (b) The emission spectrum of the human body at a skin temperature of 34 °C. (c) Schematic of heat transport between the human body, textile, and ambient environment.

physiological characteristics and processes as well as the environmental conditions. For example, in a sedentary situation in indoor offices, at a normal skin temperature of 34 °C, the heat loss is to a large extent (more than 50%) due to the emission of infrared (IR) radiation centered near 10 μm (see Fig. 1b). Therefore, by employing photonic concepts in textiles, one can tailor the radiative heat transfer and design temperature-regulating fabrics [6].

An effective personal thermoregulating garment should maintain the skin temperature around 34 °C, subsequently keeping the user in thermal comfort for a wider range of ambient temperatures. However, traditional textiles provide a limited comfort range with respect to temperature. For example, in cold weather, the human body's temperature is higher than the ambient, leading to heat loss. At the same time, a warm winter garment can block heat loss and warm the body. In contrast, summer clothing allows the human body to relieve heat stress in hot weather conditions. Therefore, it is not feasible to use a single fabric comfortably in both hot and cold weather; it cannot adapt to a change in ambient temperature. This can be solved by designing a fabric that can regulate heat transfer processes between the body, the air gap (i.e., microclimate), the fabric, and the ambient environment (see Fig. 1c). Concretely, if one expands the preset cooling/heating temperature range by 2 °C, this can save around 20% of the energy consumption.

Recently, various nano- to micro-sized photonic platforms and geometries have been investigated and utilized for temperature-regulating textiles [7, 8, 9]. In designing this technology one generally distinguishes two approaches: modulating the transmission through the fabric or adjusting the

emission from the fabric surface. Based on these concepts, the scientific community designed several state-of-the-art dual-mode (for both heating and cooling) fabrics with active (requires energy) or passive (requires no energy) switching capabilities. Indeed, the most attractive thermoregulating fabrics are at the same time dual-mode, dynamic and passive.

For example, Leung et al. proposed a fabric that modulates the transmittance to deliver a heating and cooling performance [10]. Zhang et al. reported carbon nanotube-coated bimorph fibers to dynamically modulate the IR emissivity, providing both cooling and heating by adapting to the relative humidity [11]. Another interesting design based on transmittance modulation was presented with a bi-layer fabric from a combination of polyethylene terephthalate and moisture-responsive yarns [12]. In previous works, we demonstrated various fabric designs with dual-mode temperature regulation capability using photonic concepts [13, 14, 15, 16].

Here, following the design directions discussed above (i.e., transmission or emission modulation), we introduce two fabric designs: a periodic micro-wire-based fabric, which modulates transmission [14], and a randomly distributed nano-wire-based fabric, which modulates emissivity. Both designs can deliver a dual-mode (cooling and heating) thermoregulating functionality by capitalizing on various thermal and photonic properties, with a dynamic switching capability via a shape memory polymer. This provides an opportunity to thermoregulate over a large range of ambient temperatures.

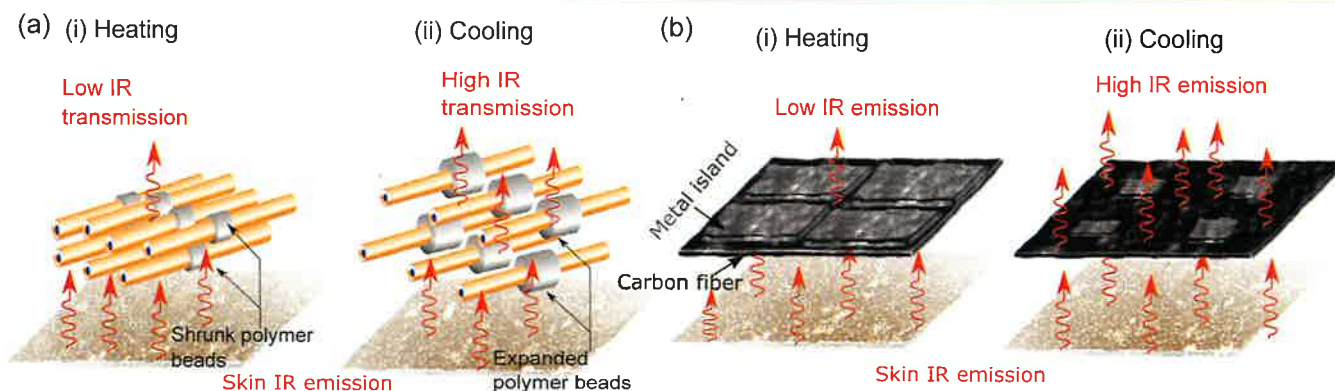


**Figure 2:** Schematic illustration of the working principle behind: (a) transmission modulating fabric (TMF), (b) emissivity modulating fabric (EMF).

## Design concepts

The first design is the transmission modulating fabric (TMF) (Fig. 2a) that incorporates fibers coated with a conductive material, which are arranged in an array in a suitable combination with a shape-memory polymer, the latter providing the dynamic functionality. Its concept builds on material properties (i.e., scattering properties of the metallic coating, thermal and mechanical properties of the polymer actuator) and geometry (i.e., shape and arrangement of the fibers). The dual-mode behavior is as follows: when the ambient temperature reduces, the polymer beads shrink, thus decreasing the separation distance between two consecutive fibers. Consequently, the IR transmittance will decrease, providing the desired heating function [Fig. 2a(i)]. Conversely, when the temperature rises, the polymer beads expand, thus increasing the inter-fiber distance. This results in a new configuration with an increased IR transmittance, providing the cooling functionality [Fig. 2a(ii)]. It is known that polymers such as bio-based polylactide urethane, polyurethane, and several other polymers possess programmable shape-memory properties around the human body temperature. Therefore, the proposed polymer beads can be made from these types of materials.

The use of metal as a coating material is due to its high reflectivity in the wavelength range of human body emission. On the contrary, the IR transmission would rapidly increase with dielectric fibers (without metal) below an optimum diameter. However, due to conductivity, metal-coated fibers act like antennae, which strongly interact with

IR radiation, even if the fiber diameter is much smaller than the wavelength. This way, a strong IR transmission control is possible, with efficient thermal body regulation, as shown later. Metals such as silver, gold, copper, and aluminum can all be used as a coating on dielectric-core fibers, which can be composed of natural or synthetic textile materials such as cotton and polyester.

The emissivity modulating fabric (EMF), the second design, comprises a highly emissive bottom layer and low emissive islands on top, which are thermo-mechanically dynamic (Fig. 2b). The islands are potentially made from temperature-sensitive shape-memory polymer nanofibers using for example, electrospinning and coated with metal, while the bottom layer is composed of a highly emissive surface such as carbon fibers. By introducing an optimized metal coating on the nanofibers, one can achieve a substantial effective emissivity contrast.

The dual-mode behavior is as follows: When the ambient is cold, the fabric is in heating mode, and the polymer expands, allowing the low-emissive islands to stretch and cover the bottom high-emissive layer, as shown in Fig. 2b(i). This increases the island-coverage factor (i.e., the ratio between the island area and the bottom layer area) and substantially lowers radiation emission to the ambient (i.e., low effective emissivity of the fabric).

When the ambient is hot, the fabric is in cooling mode, the polymer shrinks; thus, the low-emissive island surface area reduces, exposing the bottom high-emissive layer to the ambient, as shown in Fig. 2b(ii) (low island-coverage factor). This results in a higher effective emissivity of the outer surface, thus strong radiative emission to the ambient.

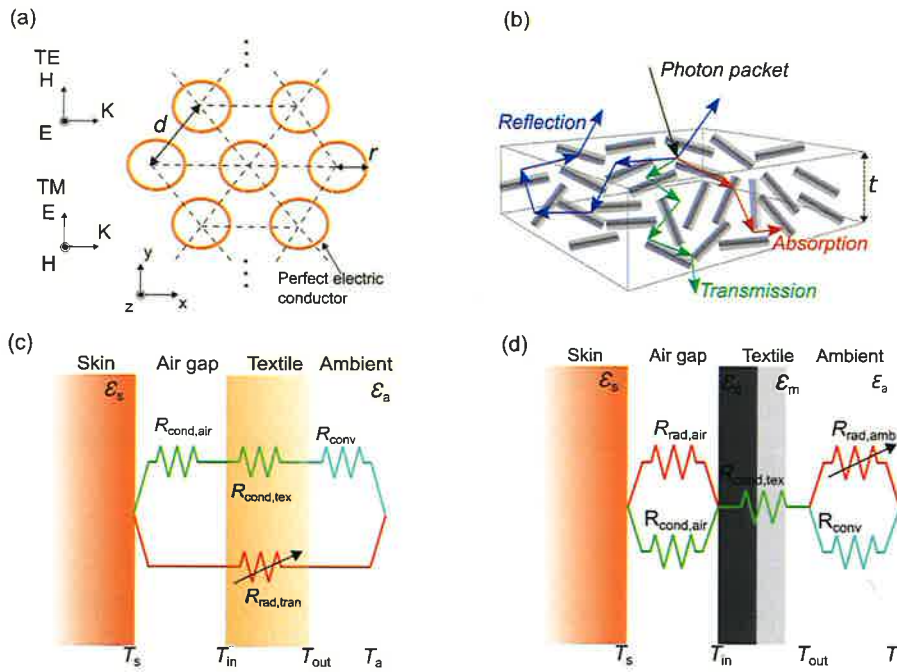


**Figure 3:** The simulation model of (a) TMF, with the polarization convention and incidence direction, the pattern is repeated in the vertical  $y$  direction and (b) EMF, with radiative transport through nanofiber-based islands. The thermal circuit analogy of the main heat-flow channels when the fabric covers the skin, with an air gap in between is shown with corresponding thermal resistances (the arrow indicates variable radiative resistance) and temperatures for (c) TMF and (d) EMF.

### Modeling methods

To understand the IR optical responses of the designs, we implemented various numerical study approaches accordingly. For the TMF fabric, we used full-wave electromagnetic simulations; for EMF, we implemented scattering theory combined with radiative transfer theory solved using Monte Carlo (MC) calculations. While the thermal modeling for both designs is implemented using circuit models.

### Electromagnetic modeling

To study the IR response of TMF, we employ the finite-element method to calculate rigorous solutions of Maxwell’s equations using commercial software (COMSOL Multiphysics). Since the fibers are considered infinitely long, the two-dimensional (2D) geometries consist of fibers arranged hexagonally (Fig. 3a). The geometry comprises metallic fibers with radius  $r$  and center-to-center distance  $d$ . In the relevant IR range (5-20  $\mu\text{m}$ ), many metals can be approximated as perfect electric conductors with infinite conductivity. Thus, we implement the Perfect Electric Conductor (PEC) boundary condition, which leads to a complete

reflection from these surfaces without any losses [14].

In the simulations, a perpendicular plane wave source impinges on the structure. The IR spectral parameters strongly depend on the polarization. Therefore, it is crucial to consider both a transverse electric (TE, one electric field component out-of-plane) and transverse magnetic (TM, one magnetic field component out-of-plane) case. Floquet periodic boundary conditions are used on the top and bottom to represent an infinite repetition in the vertical direction. The diffraction orders for smaller wavelengths are computed with Port conditions on the right and left.

### Radiative transfer modeling

To retrieve EMF’s spectral emissivity, we numerically solve the radiative transfer equation using the collision-based MC method [15]. Here, the effective optical parameters are calculated using classical Lorenze-Mie solutions for a cylinder and employed as an input in the MC simulation. A ray is characterized by its position, wavelength, and direction during its propagation throughout the medium (Fig. 3b). Each new ray is launched at the upper boundary of the medium. It may be reflected

back or enter the medium. If it enters the medium, scattering and absorption events will take place. Rays that hit the internal side of the interfaces are reflected or transmitted accordingly. If the ray is reflected back to the medium, it will go through another process of possible absorption or scattering. On the other hand, if it is transmitted through the top boundary, it will contribute to the reflectance. If it is transmitted through the bottom boundary, it contributes to transmittance. As Kirchhoff's law states, at thermodynamic equilibrium, the absorption equals the emissivity. Thus, we take the absorptance calculated using MC as emissivity.

The radiative transfer equation is solved between 5 and 20  $\mu\text{m}$  for wavelength (2971 equally spaced wavelengths) and 0–90° for angle (31 equally spaced angles).  $10^4$  photons are launched for each angle and wavelength, which corresponds to a total of  $2971 \times 31 \times 10^4 \cong 921$  million photons launched.

### Thermal modeling

The assessment of cooling and heating performance is determined by the maximum and minimum surrounding environment temperature that the fabric can maintain without affecting the wearer's thermal comfort. This is called the setpoint temperature, and one can calculate it from a heat transfer analysis e.g., using a circuit model. We treat thermal dissipation from the human body to the ambient as a one-dimensional (1D) steady-state heat transfer problem in dry conditions, hence ignoring mass transfer. This assumption holds in most indoor seating scenarios where movements are limited to sedentary activities, and occupants are not actively perspiring, with negligible sweating. We use different circuit models since TMF is a transparent (non-absorbing/non-emitting) layer, while the EMF is opaque.

For transparent (non-absorbing/non-emitting) fabric layers, such as TMF, the radiative transfer in the air gap, in the fabric, and in front of the fabric is the same. Conduction in the air gap, conduction in the fabric, and convection from the fabric surface are the other contributions [14]. For an opaque fabric layer such as EMF, radiative and conductive heat transfer constitute the exchange through the air gap, while the heat dissipation from the fabric to the ambient is via radiation and convection. Another conductive exchange contributes to heat

transfer in the textile [13].

A thermal circuit model is constructed for both cases involving the conductivity of the textile and its radiative properties, obtained from the electromagnetic simulations, as well as properties of the air gap and ambient, see Fig. 3c-d. The  $R$  symbols represent the thermal resistances, and the corresponding subscripts denote radiation in air, transmitted through the fabric and the ambient, conduction in air and the textile, and convection, respectively. Furthermore, we use the inside and outside temperatures  $T_{in}$  and  $T_{out}$ , the skin temperature  $T_s$ , and the ambient temperature  $T_a$ . The requirement for a wearer's thermal comfort is the balance between metabolic heat generation and total heat loss in dry conditions.

The total heat loss is controlled by the total thermal resistance ( $R_{tot}$ ) between skin and ambient. Due to the variable radiative thermal resistance ( $R_{rad,tran}$  for TMF and  $R_{rad,amb}$  for EMF), the total thermal resistance varies between the cooling and heating modes. Subsequently, the total heat flux through the air gap and fabric to the ambient is given by:  $Q = R_{tot}^{-1}(T_{skin} - T_{amb})$  which is assumed to be equal to a constant base metabolic body heat generation of  $70 \text{ W/m}^2$ , corresponding to a sedentary individual with a constant skin temperature of  $34 \text{ }^\circ\text{C}$ . A typical air gap thickness between the skin and fabric in moderate-fitting clothing is around 1 mm, thus, this value is taken for the microclimate thickness. Furthermore, the thermal conductivity of air is  $k_{air} = 0.03 \text{ Wm}^{-2}\text{K}^{-1}$ , and the natural convection heat transfer coefficient is  $h = 3 \text{ Wm}^{-1}\text{K}^{-1}$ . Convective heat transfer in the air gap is negligible due to the small Rayleigh number, which stems from the relatively small air gap thickness. The emissivity of the skin is approximated as a gray body with  $\epsilon_{skin} = 0.98$ , the emissivity of ambient as a black body is  $\epsilon_{amb} = 1$ .

### Results and discussion

The spectral transmittance for the TMF is presented in Fig. 4a for two different separation distances  $d$  and a filling factor ( $2r/d$ ) of 0.15. For  $d = 2 \mu\text{m}$ , starting from a cut-off wavelength of  $5 \mu\text{m}$ , there is a wide stopband sometimes called the plasmonic gap. On the other hand, for  $d = 12 \mu\text{m}$ , the first (above  $13 \mu\text{m}$ ) and second (below  $10 \mu\text{m}$ ) transmission bands are visible, while the plasmonic gap is shifted

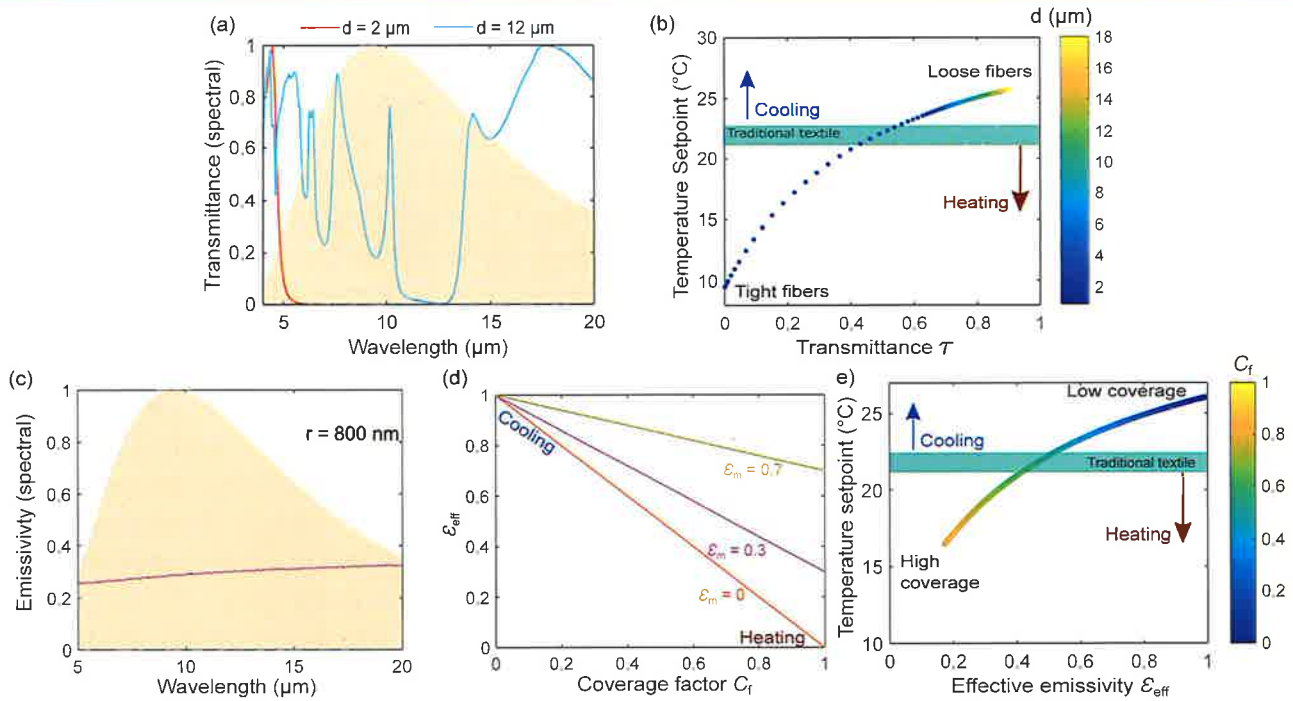


**Figure 4:** (a) TMF spectral transmittance as a function of wavelength for fiber separation distance  $d = 2$  and  $12 \mu\text{m}$ . (b) TMF ambient setpoint temperature as a function of integrated transmittance  $\tau$  and separation  $d$ . (c) EMF spectral emissivity as a function of wavelength for wire radius  $r = 800 \text{ nm}$ . (d) EMF effective emissivity  $\epsilon_{\text{eff}}$  as a function of covering factor  $C_f$  for varying metal island emissivity  $\epsilon_m = 0$  (ideal case),  $0.3$ , and  $0.7$ . (e) EMF ambient setpoint temperature as a function of  $\epsilon_{\text{eff}}$  and  $C_f$ .

to a higher wavelength (not visible on the graph). In addition to the plasmonic gap, we observe a structural band gap for wavelengths just below the first transmission band, which originates from the geometric design and extends from 10 to 14  $\mu\text{m}$ , blocking the transmission of thermal radiation. Finally, below the structural band gap, there is a continuous second transmission band below 10  $\mu\text{m}$ , with a set of resonances.

The above photonic effects are present in both spectral curves, so we can assess the influence of the separation  $d$ . When  $d$  increases, the spectral curve shifts to a longer wavelength region and vice versa, thus shifting the plasmonic gap and the first transmission band. As a result, for larger  $d$  (but not too large), both the first and second transmission bands are underneath the human body emissivity curve, leading to more transmission of IR thermal radiation from the skin to the environment. This allows the TMF to operate in a cooling mode. On the other hand, for smaller  $d$ , the plasmonic gap is underneath the human body emissivity curve. Consequently, a very low IR transfer from the skin to the environment is realized; in this case the TMF is operating in a heating mode.

As mentioned, the thermoregulating performance is based on the maximum and minimum ambient temperatures with comfort: the setpoint temperatures. The TMF achieves a minimum setpoint of  $9.5 \text{ }^\circ\text{C}$  (Fig. 4b), which corresponds to an integrated transmittance  $\tau$  close to zero where  $d = 1.2 \mu\text{m}$  (expected maximum shrinking limit of polymer beads), and the plasmonic gap covers most of the human body emissivity curve; thus, the fabric is opaque to thermal radiation emitted by the human body. On the other hand, a maximum setpoint of  $25.7 \text{ }^\circ\text{C}$  is feasible, which corresponds to spectrally integrated  $\tau = 0.9$ , where  $d = 14 \mu\text{m}$  (expected maximum swelling limit of polymer beads). Then, the second transmission band is the dominant photonic effect under the human body emissivity curve, leading to a highly transparent fabric for thermal radiation emitted by the body (Fig. 4b).

For EMF, the spectral emissivity of the metal islands comprised of a cloud of randomly distributed nano-wires is displayed in Fig. 4c. One observes more or less a low and constant emissivity over the body emissivity range. The thickness ( $t$ ) of the metal islands is  $200 \mu\text{m}$ , while the nano-wire radius

( $r$ ) is 800 nm. The human body emissivity curve (skin at 34 °C) is plotted for comparison (orange background). The total integrated emissivity is about 0.3. Figure 4d shows the effective emissivity  $\varepsilon_{\text{eff}}$  as a function of the covering factor  $C_f$  for three different situations: where the metal island has a total emissivity  $\varepsilon_m$  of 0 (perfect reflector, ideal case), 0.3 (the case for  $r = 800$  nm, spectrally integrated value of Fig. 4c), and 0.7 (a case where the island nanowires reflect/scatter less).

For high coverage  $C_f$ , the effective emissivity is low due to the complete coverage of the bottom highly emissive layer by the top metallic layer. Thus, radiative transfer to the ambient is substantially reduced, and the design is in heating mode. For the highest covering factor ( $C_f = 1$ ), the effective emissivity will have the same value as the emissivity of the metallic islands, for example, 0, 0.3, and 0.7 in Fig. 4d. While for low coverage  $C_f$ , meaning a large area of the bottom layer is exposed to the ambient, independent of the emissivity of the metal islands, the effective emissivity is 1 (ideal case). This is facilitated by shrunken metallic islands, so in this scenario, the EMF will emit radiation to the ambient and provide a cooling functionality.

From the heat transfer analysis, with all necessary parameters, we retrieve the setpoint temperature that the EMF can achieve, see Fig. 4e (the color bar indicates the effect of  $C_f$ ). By utilizing a fiber radius of about 800 nm the EMF design can attain a 26 °C highest setpoint temperature in cooling mode ( $\varepsilon_{\text{eff}} = 1$ ) and a 16 °C lowest setpoint temperature ( $\varepsilon_{\text{eff}} = 0.2$ ). As a result, there is a very large and useful thermal comfort setpoint window of 10 °C.

According to the setpoint temperature values, one can conclude that the TMF design performs better for heating functionality (with a lowest setpoint temperature of 9.5 °C), while EMF performs better for cooling functionality (with a highest setpoint temperature of 26 °C). With respect to comfort range, the TMF provides the better performance, with about 16 °C window compared to EMF with 10 °C.

We compare the performance of the proposed fabric designs with other existing technologies: For the TMF design, the lowest setpoint is 11.1 °C lower than for the Omni-Heat technology (20.6 °C) [17], 4.8 °C lower than for the Mylar/space blanket (14.3 °C) [18], 4.4 °C lower than for the dual-mode textile (13.9 °C) [19], 5.2 °C lower than for the

nanoporous metalized polyethylene textile (14.7 °C) in its cotton/polyethylene/Ag configuration [20]. For the EMF design, the lowest setpoint is 4.6 °C lower than for Omni-Heat technology (20.6 °C) [17] and 6.8 °C lower than for cotton (22.8 °C). Furthermore, the highest setpoint for TMF and EMF is 2.9 °C and 3.2 °C larger than that of cotton (22.8 °C), 1.4 °C and 1.7 °C more than for the dual-mode textile (24.3 °C) [19]. In essence, our designs are promising and capable of preserving the thermal comfort of the wearer in a highly dynamic temperature situation.

## Conclusion

Thermal comfort is an important human sensation with clothing as the main means to achieve it. In general, textiles control the heat transfer from the body to the ambient to ensure thermal balance and comfort. However, traditional textiles are insufficient, and external heating and cooling systems are used. Furthermore, the energy spent for (mostly empty) spaces of buildings becomes an enormous drain. Traditional textiles can only function in one mode and are usable in a limited temperature window. Therefore, one must adapt the clothing to different conditions: warming textiles for cold surroundings and cooling textiles in warm environments.

To address these problems, we propose fabric designs for personal thermal regulation based on photonic engineering. The designs possess dual-mode functionality (cooling and heating) with a switching capability facilitated via a shape memory polymer. Extensive electromagnetic and thermal modeling is implemented to demonstrate the potential thermoregulating benefits. In general, our designs provide an opportunity to thermoregulate over a wide range of ambient temperatures and they demonstrate a large potential for replacing current heating and cooling systems, which allows substantial energy savings and assists in the path to a sustainable future.

## Acknowledgments

Funding via the INTERREG PHOTONITEX and ARC-21/25 UMONS2 projects, and a postdoctoral fellowship from the FNRS. The authors thank Gilles

Rosolen, Alice De Corte and the colleagues from the PHOTONITEX project for fruitful collaborations.

## References

- [1] Beerepoot, M. and Marmion, A., "Policies for renewable heat: An integrated approach," Tech. Rep., OECD Publishing (2012).
- [2] Andre, T. and Guerra F., "Renewables 2020 global status report," *Rep. Paris: REN12* (2020).
- [3] McMichael, A. J., Woodruff, R. E., and Hales, S., "Climate change and human health: present and future risks," *The Lancet* 367(9513), 859–869 (2006).
- [4] Peng, Y. and Cui, Y., "Advanced textiles for personal thermal management and energy," *Joule* 4(4), 724–742 (2020).
- [5] Andre, M., De Vecchi, R., and Lamberts, R., "User-centered environmental control: a review of current findings on personal conditioning systems and personal comfort models," *Energy and Buildings* 222, 110011 (2020).
- [6] Zuo, X., Zhang, X., Qu, L., and Miao, J., "Smart fibers and textiles for personal thermal management in emerging wearable applications," *Advanced Materials Technologies*, 2201137 (2022).
- [7] Fang, Y., Chen, G., Bick, M., and Chen, J., "Smart textiles for personalized thermoregulation," *Chemical Society Reviews* (2021).
- [8] Tabor, J., Chatterjee, K., and Ghosh, T. K., "Smart textile-based personal thermal comfort systems: current status and potential solutions," *Advanced Materials Technologies* 5(5), 1901155 (2020).
- [9] Lan, X., Wang, Y., Peng, J., Si, Y., Ren, J., Ding, B., and Li, B., "Designing heat transfer pathways for advanced thermoregulatory textiles," *Materials Today Physics* 17, 100342 (2021).
- [10] Leung, E. M., Colorado Escobar, M., Stiubianu, G. T., Jim, S. R., Vyatskikh, A. L., Feng, Z., Garner, N., Patel, P., Naughton, K. L., Follador, M., Karshalev, E., Trexler, M. D., and Gorodetsky, A. A., "A dynamic thermoregulatory material inspired by squid skin," *Nature communications* 10(1), 1947 (2019).
- [11] Zhang, X. A., Yu, S., Xu, B., Li, M., Peng, Z., Wang, Y., Deng, S., Wu, X., Wu, Z., Ouyang, M., and wang, Y., "Dynamic gating of infrared radiation in a textile," *Science* 363(6427), 619–623 (2019).
- [12] Fu, K., Yang, Z., Pei, Y., Wang, Y., Xu, B., Wang, Y., Yang, B., and Hu, L., "Designing textile architectures for high energy-efficiency human body sweat-and cooling-management," *Advanced Fiber Materials* 1(1), 61–70 (2019).
- [13] Abebe, M. G., De Corte, A., Rosolen, G., and Maes, B., "Janus-yarn fabric for dual-mode radiative heat management," *Physical Review Applied* 16(5), 054013 (2021).
- [14] Abebe, M. G., Rosolen, G., Khouzakoun, E., Odent, J., Raquez, J.-M., Desprez, S., and Maes, B., "Dynamic thermal-regulating textiles with metallic fibers based on a switchable transmittance," *Physical Review Applied* 14(4), 044030 (2020).
- [15] Abebe, M. G., Rosolen, G., Odent, J., Raquez, J.-M., and Maes, B., "A dynamic passive thermoregulation fabric using metallic microparticles," *Nanoscale* 14(4), 1421–1431 (2022).
- [16] Altamirano, M. G., Abebe, M. G., Hergué, N., Lejeune, J., Cayla, A., Campagne, C., Maes, B., Devaux, E., Odent, J., and Raquez, J., "Environmentally responsive hydrogel composites for dynamic body thermoregulation," *Soft Matter* 19(13), 2360–2369 (2023).
- [17] Hayes, S. G. and Venkatraman, P., *Materials and technology for sportswear and performance apparel*, CRC Press Boca Raton (2016).
- [18] McCann, J. D., *Build the Perfect Survival Kit*, Penguin (2013).
- [19] Hsu, P.-C., Liu, C., Song, A. Y., Zhang, Z., Peng, Y., Xie, J., Liu, K., Wu, C.-L., Catrysse, P. B., Cai, L., et al., "A dual-mode textile for human



body radiative heating and cooling," *Science Advances* **3**(11), e1700895 (2017).

- [20] Cai, L., Song, A. Y., Wu, P., Hsu, P.-C., Peng, Y., Chen, J., Liu, C., Catrysse, P. B., Liu, Y., Yang, A., et al., "Warming up human body by nanoporous metallized polyethylene textile," *Nature communications* **8**(1), 1–8 (2017).